Electrical components library for HAWC2

Cutululis, Nicolaos Antonio; Larsen, Torben J.; Sørensen, Poul Ejnar; Iov, F.; Hansen, Anca Daniela

Publication date:
2007

Document Version
Publisher's PDF, also known as Version of record

Risø-R-Report

Electrical Components Library for HAWC2

Nicolaos A. Cutululis, Torben J. Larsen,
Poul Sørensen, Florin Iov, Anca D. Hansen

Risø-R-1587(EN)

Risø National Laboratory
Technical University of Denmark
Roskilde, Denmark
December 2007

Author: Nicolaos A. Cutululis, Torben J. Larsen, Poul Sørensen, Florin Iov[*], Anca D. Hansen
Title: Electrical Components Library for HAWC2
Department: Wind Energy Department
[*]Aalborg University, Institute of Energy Technology

Risø-R-1587(EN)
December 2007

Abstract (max. 2000 char.):

The work presented in this report is part of the EFP project called "A Simulation Platform to Model, Optimize and Design Wind Turbines" partly funded by the Danish Energy Authority under contract number 1363/04-0008. The project is carried out in cooperation between Risø National Laboratory and Aalborg University.

In this project, the focus is on the development of a simulation platform for wind turbine systems using different simulation tools.

This report presents the electric component library developed for use in the aeroelastic code HAWC2. The developed library includes both steady state and dynamical models for fixed and variable speed wind turbines.

A simple steady-state slip model was developed for the fixed speed wind turbine. This model is suitable for aeroelastic design of wind turbines under normal operation.

A dynamic model of an induction generator for the fixed speed wind turbine was developed. The model includes the dynamics of the rotor fluxes. The model is suitable for a more detailed investigation of the mechanical – electrical interaction, both under normal and fault operation. For the variable speed wind turbine, a steady-state model, typically used in aeroelastic design, was implemented. The model can be used for normal and, to some extent, for fault operation. The reduced order dynamic model of a DFIG was implemented. The model includes only the active power controller and can be used for normal operation conditions.

ISSN 0106-2840
ISBN 978-87-550-3573-7

Contract no.:
ENS 1363/04-0008

Group's own reg. no.:
1115043-00

Sponsorship:
Danish Energy Authority

Cover :

Pages: 35
Tables:
References: 17

Information Service Department
Risø National Laboratory
Technical University of Denmark
P.O.Box 49
DK-4000 Roskilde
Denmark
Telephone +45 46774004
bibl@risoe.dk
Fax +45 46774013
www.risoe.dk

Contents

Preface

The work presented in this report is part of the EFP project called “A Simulation Platform to Model, Optimize and Design Wind Turbines” partly funded by the Danish Energy Authority under contract number 1363/04-0008. The project is carried out in cooperation between Risø National Laboratory and Aalborg University.

1 Introduction

The present report describes the electrical components library developed and implemented in the aero elastic code HAWC. The development of these models in HAWC is part of the results of a national Danish research project, whose overall objective is to create a model database of models for wind turbines electrical components mainly, in different simulation tools in order to enhance the design and optimization of wind turbines.

The simulation tools used in this project are MATLAB/Simulink, Saber, DIgSILENT (Power Factory) and HAWC. MATLAB® has been used in this project as a general developer tool for the other simulation tools. Saber is a simulation tool used in circuit and power electronics design including electrical, thermal, magnetic and mechanical components, while Power Factory is a dedicated electrical power system simulation tool used for assessment of power quality and analysis of the wind turbine interaction with the grid. All these tools use simplified aerodynamic and mechanical models for the wind turbine. On the other hand Horizontal Axis Wind turbine Code (HAWC) [1], is a code developed for calculating wind turbine response in time domain. It contains a very detailed description of the aero elastical and mechanical aspects existing within a wind turbine. Its main purpose is the calculation of dynamic loads on the structure.

Even if HAWC is very detailed on the structural dynamics, using a finite element model of the wind turbine simple generator models are typically used. In most of the cases the generator is represented as a damping, which is essentially a linearization of the steady state torque-speed relation of the 1^{st} order model. This linearization is reasonable only for small slip values corresponding to the normal operation range of a Squirrel-Cage Induction Generator (SCIG) in wind turbine applications. Still, even in the normal slip range the non-linearity has some influence on the damping effect of the generator, because the damping decreases when the slip (absolute value) increases. Thus, the non-linear steady-state representation is relevant, also for wind turbine applications in the normal slip operation range.

Larsen et. al. [2] extended the HAWC code with generator dynamics corresponding to the 5^{th} order model, i.e. including stator as well as rotor flux transients. The code can also simulate with the 1^{st} order model and the 3^{rd} order model. Simulations with the complete structural model combined with full generator dynamics of a SCIG indicate that there is a risk for coupling between the generator eigenfrequency [2] and structural modes of the wind turbine. It is confirmed that generator dynamics can be essential, even in normal operation of the wind turbine, assuming an ideal power system with constant grid voltage on the generator terminals.

Furthermore, with the new grid connection requirements for wind turbines where the power plant wind turbines participate actively in the stabilization of power systems, the investigations of the fatigue and extreme loads of wind turbines become more and more important. Especially the requirements for wind turbines to stay connected to the grid during and after voltage sag imply potential challenges in the design of wind turbines, both for mechanical structure and electrical system. Thus, it is very important to develop models of the electrical components that can be used in aero elastic codes and allow to quantify the loads' impact on the wind turbines' lifetime, during and after grid faults.

The aero elastic simulation tool HAWC has been replaced by HAWC2, a new and improved aero elastic simulation tool, developed at the aerolastic design research programme in the Wind Energy Department of the Risø National Laboratory.

The electrical component library presented in the report contains steady – state and dynamic models for fixed and variable speed wind turbines.

The report is organised as follows. First, a short overview of the aeroelastic code HAWC2 is presented. The steady – state and the dynamic generator models, for fixed speed wind turbines, are presented in Chapter 3. Chapter 4 deals with the steady – state and dynamic models for a variable speed wind turbine. The performance of the generator models developed in HAWC2 is assessed and discussed by means of simulations. Finally, some concluding remarks, along with directions for future development, end this report.

2 HAWC2

2.1 An overview

The aero elastic simulation tool HAWC2 (***H****orizontal* ***A****xis* ***W****ind turbine simulation* ***C****ode*) is a code designed for calculating wind turbine response in time domain. It has been developed at the aeroelastic design research programme in the Wind Energy Department of the Risø National Laboratory.

The structural part of the code is based on a multibody formulation. In this formulation the wind turbine main structures is subdivided into a number of bodies where each body is an assembly of Timoshenko beam elements. Each body includes its own coordinate system with calculation of internal inertia loads when this coordinate system is moved in space, hence large rotation and translation of the body motion is accounted for. Inside a body the formulation is linear, assuming small deflections and rotations. This means that a blade modelled as a single body will not include the same nonlinear geometric effects related to large deflections as a blade divided into several bodies. The bodies representing the mechanical part of the turbine are connected by joints also referred to as constraints. The constraints are formulated as algebraic equations that impose limitations of the bodies' motion. This could in principal be a trajectory the body needs to follow, but related to the wind turbine implementation there are so far the possibility of a fixed connection to a global point (e.g. tower bottom clamping), a fixed coupling of the relative motion (e.g. fixed pitch, yaw), a frictionless bearing and a bearing where the rotation angle is controlled by the user. It may be worth to notice, that also for the last constraint where the rotation is specified, inertial forces related to this movement is accounted for in the response.

External forces are in general placed on the structure in the deformed state, which is especially important for pitch loads and twist of the blades and since large rotations are handled by a proper subdivision of bodies, the code is also especially suited for calculations on very flexible turbines subjected to e.g. large blade deflections. The aerodynamic part of the code is based on the blade element momentum theory, but extended from the classic approach to handle dynamic inflow, dynamic stall, skew inflow, shear effects on the induction and effects from large deflections. One example is the effect of large flapwise blade deflections causing a change in the effective rotor diameter and that the blade forces are no longer perpendicular to the rotor plane. This reduces the thrust on the rotor thereby changing the induced velocities and vice versa.

Two dynamic stall models have been implemented where the first is generally known as the Øye [3] model, which includes the effect of stall separation lag. The second model is a modified Beddoes-Leishmann [4] model that includes the effects of shed vorticity from the trailing edge (Theodorsen Theory), as well as the effects of stall separation lag caused by an instationary trailing edge separation point. These effects are especially important related to flutter analysis, but also generally to calculate loads and stability of blades with very low torsion stiffness.

The hydrodynamic loads are based on the, within offshore technology well-known, Morison's equation. The wave kinematics are not calculated within the HAWC2 code but provided externally through a defined DLL (Dynamic Link Library) interface [5].

The wind conditions are divided into deterministic and stochastic wind. The deterministic wind is mean wind velocity, wind steps, ramps, special gust events, special shears including the possibility for fully user defined shears. The stochastic wind normally referred to as turbulence is generated outside the HAWC2 code. In the HAWC2 code two formats for reading turbulence data are possible. One is in Cartesian coordinates (e.g. Mann turbulence [6] generated by the code WAsP engineering [7]) and the other is in polar coordinates (the Veers model [8] used by FLEX5). Tower shadow effects are also a part of the wind module as it changes the wind conditions locally near the tower. For upwind turbines a potential flow method is used whereas a jet-model produces much better results for downwind turbines.

Control of the turbine is performed through one or more DLL's. The format for these DLL's is very general, which means that any possible output sensor normally used for data file output can also be used as a sensor to the DLL. This allows the same DLL format to be used whether a control of a bearing angle, an external force or moment is submitted to the structure.

The main idea of the DLL is to implement the electrical components and the control into a few procedures that can be called by HAWC2 [5]. A standard DLL library for HAWC2 would include the generator model, along with the pitch control and actuator. In Figure 1 the external component library principle is illustrated. Each component can be a separate DLL or they can be subroutines in the same DLL. The communication between the different components can be done through HAWC2 or directly between the components.

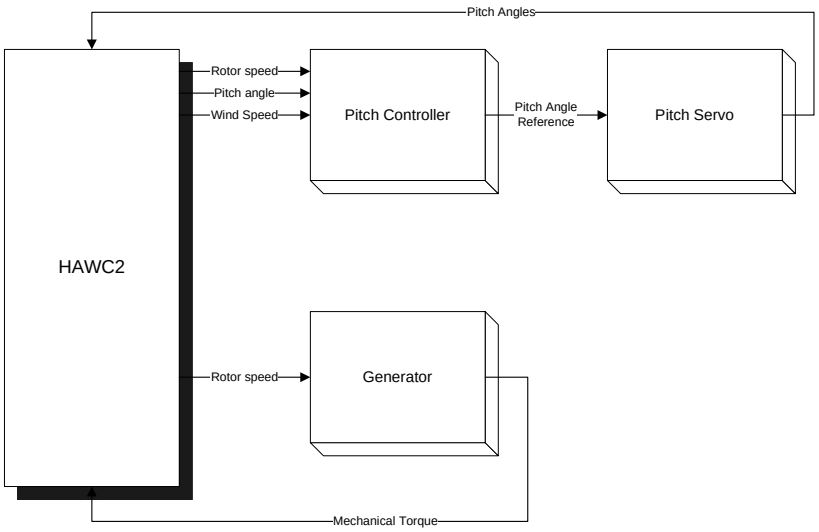

Figure 1 Block diagram of the DLL principle

An important feature of the HAWC2 code is the possibility to call different DLLs with different sample frequency, i.e. the *Pitch Controller* routine operates with a sample frequency of 10Hz, while the *Generator* and *Pitch Servo* routines operate with the normal HAWC2 step of 32-50Hz. Of course, there can be a different step for each routine.

Outputs from the code can be written to result files in either ASCII format or a more compressed binary format. It is also possible to write a special binary output file which can afterwards be used to animate the turbine behaviour.

The code has internally at Risø been tested against the older validated code HAWC. Further on a detailed verification is at the moment performed in the IEA Annex 23 [9] research project and the European UPWIND project [10]. So far these simulations cover a 5MW pitch regulated turbine at land and off-shore, on a monopole, subjected to hydrodynamic loading. The calculation time is approximately a factor of 2 slower than real time on a 3GHz CPU, which is obtained using a Newmark beta solution scheme together with Newton-Raphson iterations within each time-step. The code is limited to Windows 32 primarily caused by its use of DLL's. The source code is not public, but through the general DLL interface a lot of external coding can be performed by the user. These possibilities will be further expanded in the future.

At the moment a Windows based HAWC2 preprocessor is being developed. This should in the first edition enable the user to perform a number of quality checks of the used data. More features will be added later on.

The HAWC2 input format is written in a form that forces the user to write the input commands in a structured way so aerodynamic commands are kept together; structural commands the same, etc.

2.2 Turbine modelling

The wind turbine model implemented in HAWC2 is a generic 2MW wind turbine.

The structural part of the wind turbine has three main components, namely the tower, shaft and blades, as presented in Figure 2.

The tower is composed of 10 uniformly distributed Timoshenko beams. The shaft is composed of three beams. The generator inertia is equally distributed over the first beam, identified as the grey one in Figure 2. Each blade is divided into 4 bodies and each body composes of 23 beams.

The wind turbine hub is not modelled explicitly but is included in the blades. Thus, the blades are connected directly to the shaft through a bearing in which the rotation angle is controlled by the pitch controller/servo.

The tower top element is connected to the first element (the one bearing the generator inertia) of the shaft through a frictionless bearing. The remaining hub mass of the nacelle is placed at the top element on the tower.

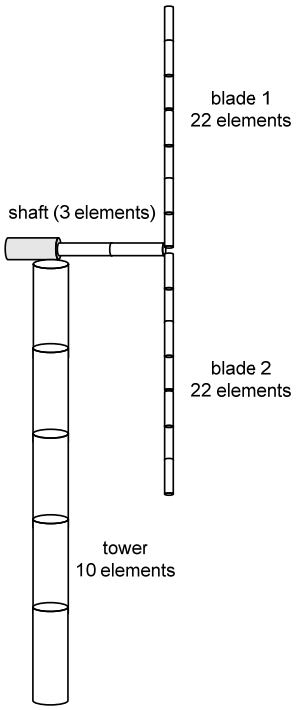

Figure 2 Wind turbine structural model

3 Wind Turbine Concepts

3.1 Fixed speed wind turbine

Fixed speed wind turbines were the most installed wind turbines in the early 1990s in combination with stall controlled rotors. They are equipped with a squirrel cage induction generator connected directly to the grid, a soft-starter and a capacitor bank for reduction of reactive power consumption, see Figure 3. Regardless of the wind speed, the wind turbine rotor speed is almost fixed, stuck to the grid frequency, and cannot be changed. In this respect the grid behaves like a large flywheel holding the rotor speed of the turbine nearly constant irrespective of changes in wind speed. A fixed speed wind turbine has the advantages of being simple, robust, reliable and well proven and using low-cost electrical parts. Its direct drawbacks are uncontrollable reactive power consumption, mechanical stress and limited power quality control [11].

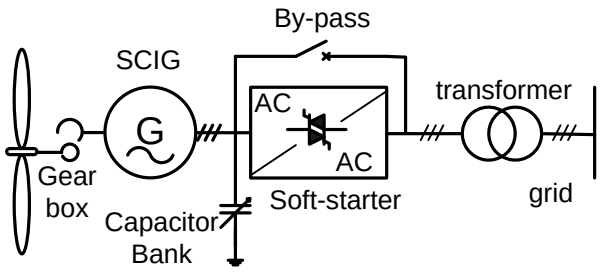

Figure 3 Fixed speed wind turbine concept

Fixed speed wind turbines can be stall or active stall wind turbines. An active stall wind turbine is in principle a stall-controlled turbine with variable pitch angle. The main difference between stall and active stall turbines is a pitch actuator system for variable pitch angles, which allows the stall effect to be controlled. In addition the power coefficient C_p can be optimised to a certain extend.

The implementation of the controller is done in a general way so that as much as possible is expressed in terms of parameters. The idea is to use this controller model to simulate different existing wind turbines with specific parameters. In-depth knowledge about manufacturer specific controller design is not necessary.

The model described in this report spans the power control during normal operation in the range from start-up wind speed to shutdown wind speed of a single speed generator turbine.

When the wind speed is between start-up wind speed and nominal wind speed the pitch angle is adjusted to optimise C_p i.e. power output.

When the wind speed is above nominal wind speed power output is limited to nominal power by utilising the stall effect. To get a flat power curve, i.e. constant nominal power in the range between nominal wind speed and shut-down wind speed, the pitch angle has to be adjusted accordingly. The maximal power of a stall turbine depends on air density, grid frequency and aerodynamic influences e.g. dirt on the blades.

Figure 4 shows the power curves for fixed speed – passive and active stall – wind turbine, as well as the power curve of variable speed wind turbines.

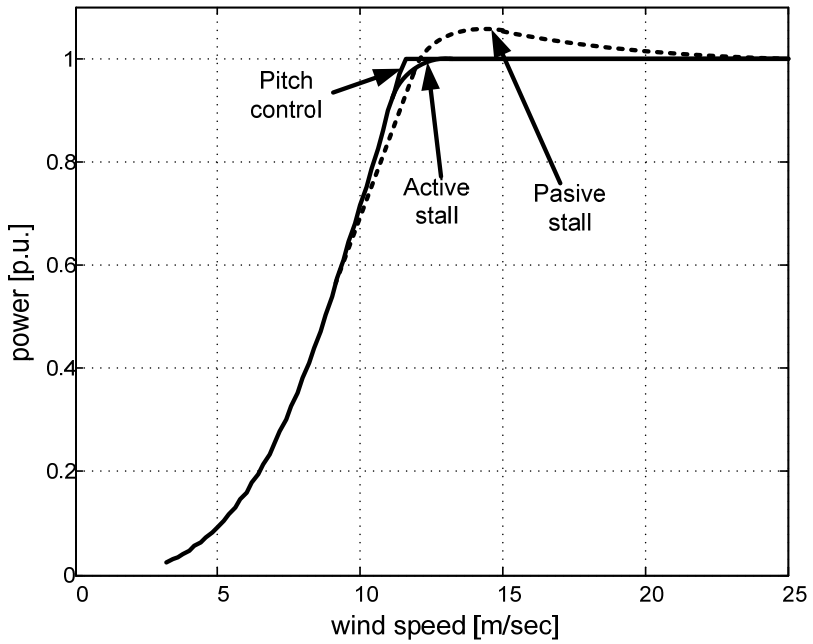

Figure 4 Typical power curves for fixed speed (passive and active stall) and variable speed wind turbine

It is desirable to be able to control the electrical output power of wind turbines. There are different types of wind turbines, which apply different control strategies for controlling the output power of the turbine. One is the active stall controlled wind turbine.

The operation of an active stall wind turbine can be divided into two modes:

- Power limitation: power output is limited to nominal power when wind speed is between nominal wind speed and shut-down wind speed; pitch angle θ is adjusted to control the stall effect. In order to get a flat power curve, i.e. constant nominal power in the range between nominal wind speed and shut-down wind speed, the pitch angle has to be adjusted accordingly.
- Power optimisation: power yield is maximised between start-up wind speed and nominal wind speed; pitch angle θ is adjusted to optimise the power coefficient C_p and hence the power output.

In a passive stall turbine the pitch angle is fixed and that means that the power output can neither be optimised nor controlled limited at wind speeds beyond nominal wind speeds. Instead the stall effect leads to a drop below nominal power in the range of high wind speed.

Although active stall turbines also use the stall effect like passive stall wind turbines, active stall turbines have considerable advantages. The maximum power output of passive stall turbines depends on wind speed, air density, grid frequency, and aerodynamic influences like dirt on the blades, while the maximum power output of active stall turbines can be controlled to a constant value.

3.2 Variable speed wind turbine

During the last few years, variable speed wind turbines have become the most dominating type of yearly installed wind turbines [12]. The increased interest in variable speed wind turbines is due to their very attractive features, given by the presence of the power converter, with respect to both the wind turbine itself as well as to more onerous grid requirements.

The variable speed wind turbines are typically equipped with an induction or synchronous generator and a power converter, which makes the variable operation possible. They have a more complicated electrical system, compared to the fixed speed wind turbines. The variable speed wind turbines can therefore be designed to achieve maximum power coefficient over a wide range of wind speeds.

The power converter permits the decoupling between the generator speed and the grid, controls the generator speed in such a way that the power fluctuations caused by wind variations are more or less absorbed by changing the generator speed and implicitly the wind turbine rotor speed.

A wind turbine is characterized by its power speed characteristics. For a horizontal axis wind turbine, the amount of mechanical power P_{mec} that a turbine produces in steady state is given by [13]:

$$P_{mec} = \frac{1}{2} \rho \pi R^2 u^3 C_p(\theta, \lambda) \tag{1}$$

where ρ is the air density, R the turbine radius, u the wind speed and $C_p(\theta, \lambda)$ is the power coefficient, which for pitch controlled wind turbines depends on both the pitch angle θ and the tip speed ratio λ. The tip speed ratio λ is given by:

$$\lambda = \frac{\omega_{rot} R}{u} \tag{2}$$

where ω_{rot} denotes the rotor turbine speed.

The prime motivation for variable speed wind turbines at lower wind speeds is to adjust the rotor speed at changing wind speeds so that the power coefficient $C_p(\theta, \lambda)$ always is maintained at its maximum value and to reduce the noise emission from aerodynamic blade noise. The power coefficient $C_p(\theta, \lambda)$ has a maximum for a particular tip-speed ratio λ_{opt} and pitch angle θ_{opt}. This means that for extracting maximum power from a particular wind speed, the control strategy has to change the turbine rotor speed in such a way that the optimum tip speed ratio λ_{opt} is always obtained. The typical $C_p(\theta, \lambda)$ curves are presented in Figure 5.

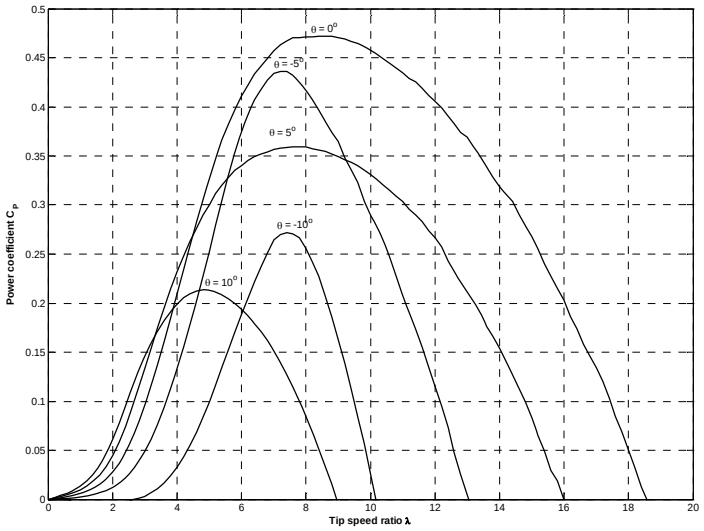

Figure 5 C_p curves for a variable speed wind turbine

The maximum power a particular wind turbine can extract from the wind is a cubic function of the turbine optimum speed, as follows:

$$P_{mec}^{\max} = K_{opt} \left[\omega_{rot}^{opt}\right]^3 \tag{3}$$

where:

$$K_{opt} = \frac{1}{2} \rho \pi R^5 \frac{C_p^{\max}}{\lambda_{opt}^3} \tag{4}$$

K_{opt} depends on the turbine characteristics and the air density. Tracking the maximum power is the goal as long as the generated power is less than the rated power. At wind speeds higher than rated wind speed, the control strategy has to be changed so that the wind turbine no longer produces maximum power but only rated power. The blades are thus pitched to reduce the power coefficient $C_p(\theta, \lambda)$ and thereby to maintain the power at its rated value. Wind gusts are absorbed by rotor speed changes using the wind turbine's rotor as short term energy storage.

The mechanical power is transformed in the generator into electrical power, the relation between them being given by:

$$P_{el} = \eta_{gen} P_{mec} \quad (5)$$

where η_{gen} is the generator efficiency.

Seen from the wind turbine point of view, the most important advantages of the variable speed operation compared to the conventional fixed speed operation are:

- reduced mechanical stress on the mechanical components such as shaft and gear-box – the high inertia of the wind turbine is used as a flywheel during gusts, i.e. the power fluctuations are absorbed in the mechanical inertia of the wind turbine.
- increased power capture – due to the variable speed feature, it is possible to continuously adapt (accelerate or decelerate) the rotational speed of the wind turbine to the wind speed, in such a way that the power coefficient is kept at its maximum value.
- reduced acoustical noise – low speed operation is possible at low power conditions (lower wind speeds).

Additionally, the presence of power converters in wind turbines also provide high potential control capabilities for both large modern wind turbines and wind farms to fulfil the high technical demands imposed by the grid operators [[14]], such as:

- controllable active and reactive power (frequency and voltage control)
- quick response under transient and dynamic power system situations
- influence on network stability
- improved power quality (reduced flicker level, low harmonics filtered out and limited in-rush and short circuit currents)

All these attractive features make the variable speed wind turbine concept very popular despite some few disadvantages, such as losses in power electronics and increased installation cost due to the power converter. Currently, there are two dominating groups of variable speed wind turbine concepts on the market [14]:

- Full variable speed concept – where the generator stator is interconnected to the grid through a full-scale power converter. The generator can be synchronous (Wound Rotor Synchronous Generator or Permanent Magnet Synchronous Generator) or induction generator (Wound Rotor Induction Generator), see Figure 6.
- Limited variable speed concept – where the generator stator is connected to the grid. The rotor frequency and thus the rotor speed are controlled. The generator is a WRIG. There are two such wind turbine concepts [14]:
    - The variable generator rotor resistance concept, where the rotor is connected to an external optically controlled resistance, whose size defines the range of the variable speed (typically 0-10% above synchronous speed), see Figure 7.
    - The doubly-fed induction generator (DFIG) concept, where the rotor is controlled by a partial scale power converter, whose size defines the range of the variable speed (typically +/- 30% around synchronous speed), see Figure 8.

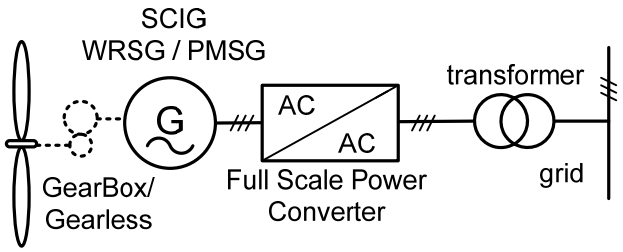

Figure 6 Variable speed wind turbine with full-scale frequency converter

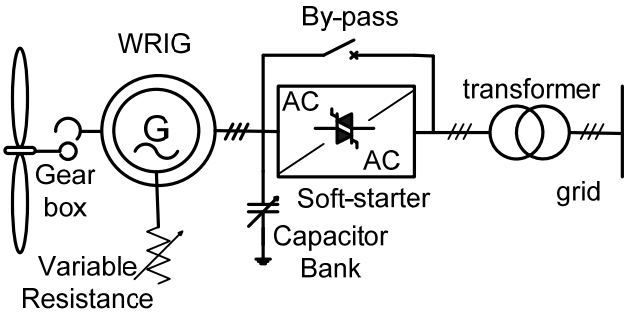

Figure 7 Variable wind speed turbine with variable rotor resistance

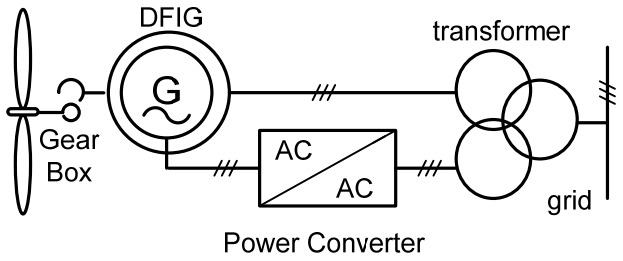

Figure 8 Variable speed wind turbine with partial-scale frequency converter

Out of all these variable speed wind turbine concepts, the concept with doubly-fed induction generator (DFIG) distinguishes itself as a very attractive option with a fast growing market demand [14]. The fundamental feature of the DFIG is that the power processed by the power converter is only a fraction of the total wind turbine power, and therefore its size, cost and losses are much smaller compared to a full-scale power converter used in the full variable speed concept.

The typical DFIG configuration, illustrated in Figure 9 consists of a wound rotor induction generator (WRIG) with the stator windings directly connected to the three-phase grid and with the rotor windings connected to a back-to-back partial scale power converter. The back-to-back converter is a bi-directional power converter. It consists of two independent controlled voltage source converters connected to a common dc-bus. These converters are illustrated in Figure 9, as rotor side converter and grid side converter. The behaviour of the generator is governed by these converters and their controllers both in normal and fault conditions. The converters control the rotor voltage in magnitude and phase angle and are therefore used for active and reactive power control.

Because the optimal voltage of the rotor is typically less than the optimal stator voltage, the transformer connecting the system to the grid has two secondaries: one winding connecting the stator and the other connecting the rotor.

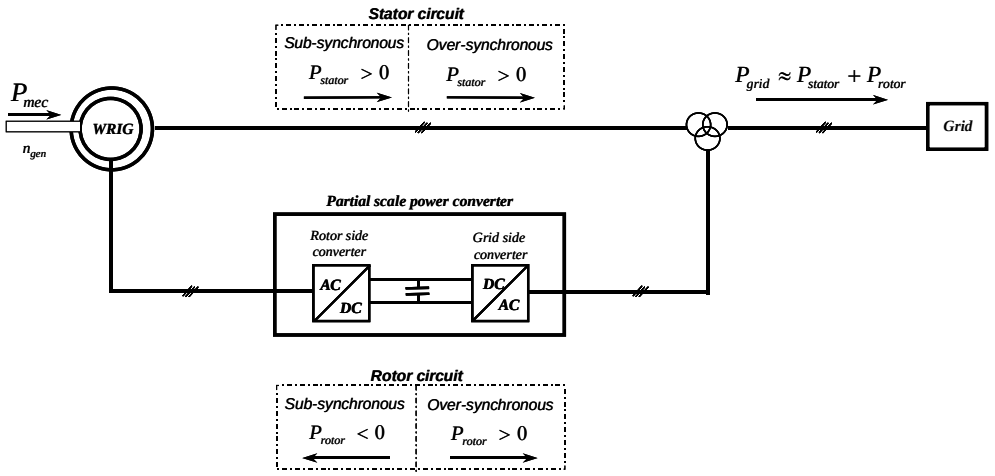

Figure 9 Principle diagram of the power flow in doubly-fed induction generator [11]

DFIG system allows variable speed operation over a large but restricted range. The smaller the operational speed range the less power has to be handled by the bi-directional power converter connected to the rotor. For example if the speed should be controllable between +/- 30%, the converter must have a rating of approximate 30% of the generator. Thus the size of the converter does not relate to the total generator power but instead to the selected speed range and hence the slip power [14]. Therefore, the cost of the power converter increases when the allowed dynamic speed range around synchronous speed increases.

Notice that, since the speed range is restricted, the slip-induced voltage is only a fraction of the grid voltage, depending on the turn-ratio between the stator and rotor. The dc bus voltage is thus relatively low. The operation at a lower dc bus voltage is possible because of the voltage reduction on the rotor side realized by the three winding transformer.

In order to cover a wide operating range from sub-synchronous to over-synchronous speed, i.e. the DFIG is able to work as a generator in both sub-synchronous (positive slip $s>0$) and over-synchronous (negative slip $s<0$) operating area, the power converter has to be able to operate with power flow in both directions. This is the reason why a back-to-back PWM (bi-directional) converter configuration is used. The slip is defined as:

$$s = \frac{n_{syn} - n_{gen}}{n_{syn}} \tag{6}$$

where n_{syn} and n_{gen} are the synchronous speed and generator speed in rpm, respectively. For a doubly-fed induction machine, it is the sign of the electrical torque, independent of the slip, which indicates if the machine is working as motor or generator.

Assuming that all the losses in the stator and rotor circuit can be neglected, the power through the power converter (through the rotor circuit), known as the slip power, can be expressed as the slip s multiplied with the stator power, P_{stator}. Furthermore, the

delivered stator power can be expressed based on the grid power P_{grid} or on the mechanical power:

$$\begin{aligned} P_{rotor} &\approx -s\, P_{stator} \\ P_{stator} &\approx P_{grid} / (1-s) = \eta_{gen}\, P_{mec} / (1-s) \end{aligned} \tag{7}$$

where η_{gen} is the generator efficiency. Depending on the operating condition of the drive, the power is fed in or out of the rotor: it is flowing from the grid via the converter to the rotor ($P_{rotor} < 0$) in sub-synchronous mode or vice versa ($P_{rotor} > 0$) in over-synchronous mode, as it is indicated in Figure 9. In both cases (sub-synchronous and over-synchronous) the stator is feeding energy to the grid ($P_{stator} > 0$) [11].

The presence of the power converter allows DFIG a more versatile and flexible operation compared with a squirrel-cage induction machine. The power converter compensates for the difference between the mechanical and electrical frequency by injecting a rotor current with a variable frequency according to the shaft speed. Through collector rings, the power converter supplies thus the rotor windings with a voltage with variable magnitude and frequency. It improves the controllable capabilities of such generator, as for example:

- it provides DFIG the ability of reactive power control. DFIG is therefore capable of producing or absorbing reactive power to or from the grid, with the purpose of voltage control (i.e. in the case of weak grid, where the voltage may fluctuate).
- it can magnetize the DFIG through the rotor circuit, independently of the grid voltage.
- it decouples active and reactive power control by independent control of the rotor excitation current.

4 Generator Modelling in HAWC2

4.1 Steady state models

4.1.1 Squirrel-cage induction generator

A simplified generator model for a squirrel-cage induction generator has been implemented. The model is based on a linear relation between slip and generator torque and assumes that the dynamics inside the generator can be approximated with a first order differential equation with a certain time constant.

The generator slip is defined as:

$$s = \frac{\omega_s - \omega_r}{\omega_s} \tag{8}$$

where ω_s is the synchronous speed of the generator and ω_r is the rotor speed of the generator. The generator torque is calculated based on the nominal torque and the ration between the actual and the nominal slip

$$T_{gen} = T_n \frac{s}{s_n} \tag{9}$$

where T_n is the nominal torque and s and s_n represent the slip and, respectively, the nominal slip.

The static generator characteristic is approximated with a linear relation as illustrated in Figure 10.

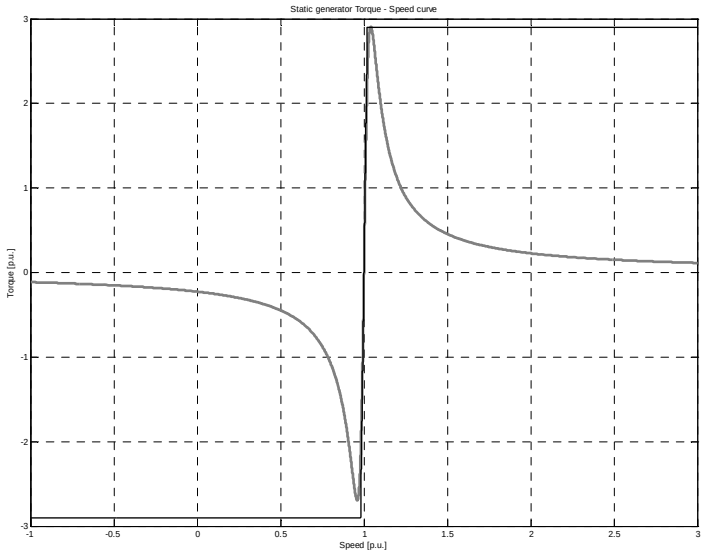

Figure 10 Slip – torque curve for an induction generator

4.1.2 Doubly-fed induction generator

The electric generator is modelled as a 1st order model, with the generator torque being a linear relation of power and speed:

$$T_{gen} = \frac{P_{ref}}{\omega} \tag{10}$$

where T_{gen} is the generator torque, P_{ref} is the reference power and ω is the generator rotor speed.

The reference power is determined from the predefined power – speed characteristic, illustrated in Figure 11, based on the filtered rotor speed. This characteristic is based on aerodynamic data of the wind turbine's rotor and its points correspond to the maximum aerodynamic efficiency.

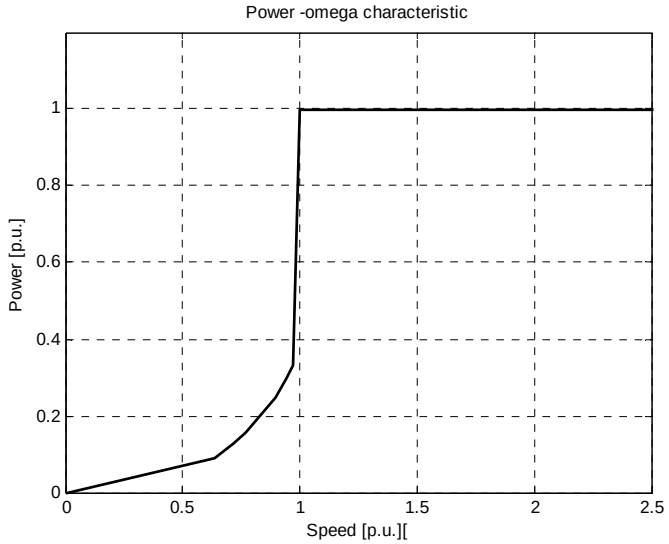

Figure 11 Power – speed characteristic

4.2 Dynamic models

4.2.1 Squirrel-cage induction generator

Full order model

Some of the machine inductances are functions of the rotor speed, whereupon the coefficients of the state-space equations (voltage equations), which describe the behaviour of the induction machine, are time-varying (except when the rotor is at stand-still). A change of variables is often used to reduce the complexity of these state-space equations. There are several changes of variables, which are used but there is just one general transformation [15]. This general transformation refers the machine variable to a frame of reference, which rotates at an arbitrary angular velocity ω_g. In this reference frame the machine windings are replaced with some equivalent windings as shown in Figure 12.

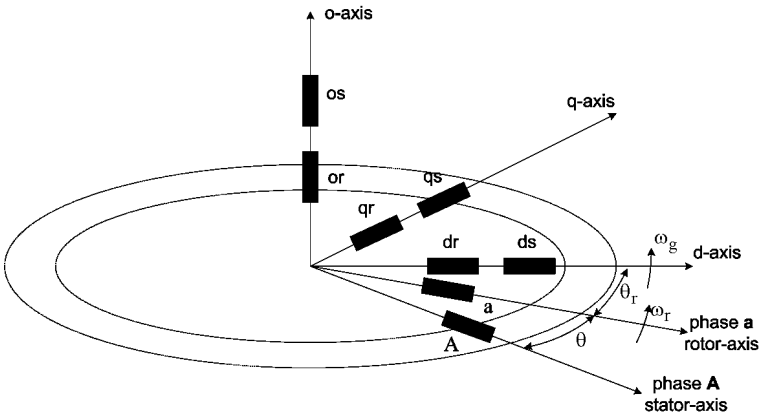

Figure 12 Induction machine windings in the dqo*-arbitrary reference frame [16]*

Using the general transformations, the voltage equations in the arbitrary reference frame can be written as:

$$\begin{bmatrix} v_{sd} \\ v_{sq} \\ v_{so} \\ v_{rd} \\ v_{rq} \\ v_{ro} \end{bmatrix} = \begin{bmatrix} R_s & & & & & \\ & R_s & & 0 & & \\ & & R_s & & & \\ & & & R_r & & \\ & 0 & & & R_r & \\ & & & & & R_r \end{bmatrix} \begin{bmatrix} i_{sd} \\ i_{sq} \\ i_{so} \\ i_{rd} \\ i_{rq} \\ i_{ro} \end{bmatrix} + \frac{d}{dt} \begin{bmatrix} \Psi_{sd} \\ \Psi_{sq} \\ \Psi_{so} \\ \Psi_{rd} \\ \Psi_{rq} \\ \Psi_{ro} \end{bmatrix} + \begin{bmatrix} 0 & -\omega_g & 0 & 0 & 0 & 0 \\ \omega_g & 0 & 0 & 0 & 0 & 0 \\ 0 & 0 & 0 & 0 & 0 & 0 \\ 0 & 0 & 0 & 0 & -(\omega_g - \omega_r) & 0 \\ 0 & 0 & 0 & (\omega_g - \omega_r) & 0 & 0 \\ 0 & 0 & 0 & 0 & 0 & 0 \end{bmatrix} \begin{bmatrix} \Psi_{sd} \\ \Psi_{sq} \\ \Psi_{so} \\ \Psi_{rd} \\ \Psi_{rq} \\ \Psi_{ro} \end{bmatrix} \tag{11}$$

where: ω_r is the electrical speed of the machine and ω_g is the speed of the general reference frame.

The compact form of (11) is:

$$[V] = [R][I] + \frac{d}{dt}[\Psi] + [\Omega][\Psi] \tag{12}$$

The relation between the linkage fluxes and the currents is given by:

$$\begin{bmatrix} \Psi_{sd} \\ \Psi_{sq} \\ \Psi_{so} \\ \Psi_{rd} \\ \Psi_{rq} \\ \Psi_{ro} \end{bmatrix} = \begin{bmatrix} L_s & 0 & 0 & L_m & 0 & 0 \\ 0 & L_s & 0 & 0 & L_m & 0 \\ 0 & 0 & L_{\sigma s} & 0 & 0 & 0 \\ L_m & 0 & 0 & L_r & 0 & 0 \\ 0 & L_m & 0 & 0 & L_r & 0 \\ 0 & 0 & 0 & 0 & 0 & L_{\sigma r} \end{bmatrix} \begin{bmatrix} i_{sd} \\ i_{sq} \\ i_{so} \\ i_{rd} \\ i_{rq} \\ i_{ro} \end{bmatrix} \tag{13}$$

or in compact form:

$$[\psi] = [L][I] \tag{14}$$

where:

- $L_m = \frac{3}{2} M_{sr}$ is the mutual inductance in the general reference frame;
- $L_s = L_{\sigma s} + L_m$ is the stator self inductance;
- $L_r = L_{\sigma r} + L_m$ is the rotor self inductance.

The voltage equations are written again in terms of currents and flux linkages. Clearly, these variables are related based on the matrix inductance $[L]$ and both cannot be independent or state variables.

If the fluxes are selected as state variables the currents can be expressed in compact form by:

$$[I] = [L]^{-1}[\Psi] \tag{15}$$

The inverse of the inductance matrix is:

$$[L]^{-1} = \frac{1}{D}\begin{bmatrix} L_r & 0 & 0 & -L_m & 0 & 0 \\ 0 & L_r & 0 & 0 & -L_m & 0 \\ 0 & 0 & \dfrac{D}{L_{\sigma r}} & 0 & 0 & 0 \\ -L_m & 0 & 0 & L_s & 0 & 0 \\ 0 & -L_m & 0 & 0 & L_s & 0 \\ 0 & 0 & 0 & 0 & 0 & \dfrac{D}{L_{\sigma s}} \end{bmatrix} \tag{16}$$

where $D = L_s L_r - L_m^2$.

After some mathematical manipulation, the state-space form of the dynamic equations (11) is:

$$\frac{d}{dt}[\Psi] = -[R][L]^{-1}[\Psi] + [V] \tag{17}$$

or in an expanded form:

$$\frac{d}{dt}\begin{bmatrix} \Psi_{sd} \\ \Psi_{sq} \\ \Psi_{so} \\ \Psi_{rd} \\ \Psi_{rq} \\ \Psi_{ro} \end{bmatrix} = -\begin{bmatrix} \dfrac{R_s L_r}{D} & -\omega_g & 0 & -\dfrac{R_s L_m}{D} & 0 & 0 \\ \omega_g & \dfrac{R_s L_r}{D} & 0 & 0 & -\dfrac{R_s L_m}{D} & 0 \\ 0 & 0 & \dfrac{R_s}{L_{\sigma s}} & 0 & 0 & 0 \\ -\dfrac{R_r L_m}{D} & 0 & 0 & \dfrac{R_r L_s}{D} & -(\omega_g - \omega_r) & 0 \\ 0 & -\dfrac{R_r L_m}{D} & 0 & (\omega_g - \omega_r) & \dfrac{R_r L_s}{D} & 0 \\ 0 & 0 & 0 & 0 & 0 & \dfrac{R_r}{L_{\sigma r}} \end{bmatrix}\begin{bmatrix} \Psi_{sd} \\ \Psi_{sq} \\ \Psi_{so} \\ \Psi_{rd} \\ \Psi_{rq} \\ \Psi_{ro} \end{bmatrix} + \begin{bmatrix} v_{sd} \\ v_{sq} \\ v_{so} \\ v_{rd} \\ v_{rq} \\ v_{ro} \end{bmatrix} \tag{18}$$

The electromagnetic torque can be obtained starting from (12) and multiplying it from the left with the transpose of the currents vector:

$$[I]^t[V] = [I]^t[R][I] + [I]^t\frac{d}{dt}[\Psi] + [I]^t[\Omega][\Psi] \tag{19}$$

where

- $P_i = [I]^t[V]$ is the instantaneous power;
- $P_{copper} = [I]^t[R][I]$ are the copper losses in the machine windings;
- $P_{mag} = [I]^t\dfrac{d[\psi]}{dt}$ is the magnetic power stored in machine (due to the variation in time of the magnetic energy);
- $P_m = [I]^t[\Omega][\Psi]$ is the mechanical power.

The electromagnetic torque is then:

$$T_e = \frac{P_m}{\Omega_r} = p\frac{P_m}{\omega_r} = \frac{3}{2}p\left(\Psi_{sd}i_{sq} - \Psi_{sq}i_{sd}\right) \tag{20}$$

where: p is the number of pole pairs and Ω_r is the mechanical speed of the rotor.

Other equivalent expressions for the electromagnetic torque of an induction machine are:

- $T_e = \frac{3}{2}p\left(\Psi_{rq}i_{rd} - \Psi_{rd}i_{rq}\right)$
- $T_e = \frac{3}{2}pL_m\left(i_{sq}i_{rd} - i_{sd}i_{rq}\right)$
- $T_e = \frac{3}{2}p\frac{L_m}{D}\left(\Psi_{sq}\Psi_{rd} - \Psi_{sd}\Psi_{rq}\right)$

The above equations may be somewhat misleading since they seem to imply that the leakage inductances are involved in the energy conversion process. This, however, is not the case. Even though the flux linkages contain the leakage inductances, they are eliminated by the algebra.

Reduced order model

The theory of neglecting electric transients is presented in [15]. For balanced steady-state operation, the variables in synchronous reference frame are constants. Hence, the electric transients of the stator can be neglected by setting the derivative of the stator fluxes in the *d* and *q* axis to zero in (11) as:

$$\begin{bmatrix} v_{sd} \\ v_{sq} \\ v_{rd} \\ v_{rq} \end{bmatrix} = \begin{bmatrix} 0 & 0 & 0 & 0 \\ 0 & 0 & 0 & 0 \\ 0 & 0 & 1 & 0 \\ 0 & 0 & 0 & 1 \end{bmatrix} \cdot \begin{bmatrix} \dot{\psi}_{sd} \\ \psi_{sq} \\ \psi_{rd} \\ \psi_{rq} \end{bmatrix} + \begin{bmatrix} \frac{R_s L_{rr}}{D} & -\omega_e & -\frac{R_s L_m}{D} & 0 \\ \omega_e & \frac{R_s L_{rr}}{D} & 0 & -\frac{R_s L_m}{D} \\ -\frac{R_r L_m}{D} & 0 & \frac{R_r L_{ss}}{D} & -(\omega_e - \omega_r) \\ 0 & -\frac{R_r L_m}{D} & (\omega_e - \omega_r) & \frac{R_r L_{ss}}{D} \end{bmatrix} \cdot \begin{bmatrix} \psi_{sd} \\ \psi_{sq} \\ \psi_{rd} \\ \psi_{rq} \end{bmatrix} \tag{21}$$

In order to avoid the computational problems due to algebraic loops (21) should be written in state space form only in terms of the rotor fluxes as [16]:

$$\begin{bmatrix} \dot{\psi}_{rd} \\ \psi_{rq} \end{bmatrix} = \begin{bmatrix} \left(\alpha\tau_{rm}\sigma_r - \frac{\tau_{rm}}{\sigma_s}\right) & \left(\left(\frac{\alpha\tau_{rm}}{\tau_{sr}}L_m + 1\right) + \omega_e - \omega_r\right) \\ -\left(\left(\frac{\alpha\tau_{rm}}{\tau_{sr}}L_m + 1\right) + \omega_e - \omega_r\right) & \alpha\tau_{rm}\sigma_r - \frac{\tau_{rm}}{\sigma_s} \end{bmatrix} \begin{bmatrix} \psi_{rd} \\ \psi_{rq} \end{bmatrix} + \begin{bmatrix} \frac{\alpha\tau_{rm}}{\tau_{sr}} & \frac{\alpha\tau_{rm}}{\tau_{sr}^2} & 1 & 0 \\ -\frac{\alpha\tau_{rm}}{\tau_{sr}^2} & \frac{\alpha\tau_{rm}}{\tau_{sr}} & 0 & 1 \end{bmatrix} \begin{bmatrix} v_{sd} \\ v_{sq} \\ v_{rd} \\ v_{rq} \end{bmatrix} \tag{22}$$

where: $\tau_{sr} = \frac{R_s L_{rr}}{D}$, $\tau_{rm} = \frac{R_r L_m}{D}$, $\sigma_r = \frac{L_m}{L_{rr}}$, $\sigma_s = \frac{L_m}{L_{ss}}$, $\alpha = \frac{1}{1 + \left(\frac{\omega_e}{\tau_{sr}}\right)^2}$.

Based on rotor fluxes and input voltages the stator fluxes can be obtained using (16):

$$\begin{bmatrix}\Psi_{sd}\\ \Psi_{sq}\end{bmatrix}=\begin{bmatrix}\alpha\sigma_r & \frac{\alpha}{\tau_{sr}}L_m\omega_e\\ -\frac{\alpha}{\tau_{sr}}L_m\omega_e & \alpha\sigma_r\end{bmatrix}\begin{bmatrix}\psi_{rd}\\ \psi_{rq}\end{bmatrix}+\begin{bmatrix}\frac{\alpha}{\tau_{sr}} & \frac{\alpha}{\tau^2_{sr}}\omega_e\\ -\frac{\alpha}{\tau^2_{sr}}\omega_e & \frac{\alpha}{\tau_{sr}}\end{bmatrix}\begin{bmatrix}v_{sd}\\ v_{sq}\end{bmatrix} \quad (23)$$

Then the electromagnetic torque is calculated based on:

$$T_e=\frac{3}{2}p\cdot\frac{L_m}{D}(\psi_{sq}\cdot\psi_{rd}-\psi_{rq}\cdot\psi_{sd}) \quad (24)$$

4.2.2 Doubly-fed induction generator model

The main idea is to provide a simple generator model which is sufficiently accurate to simulate normal wind turbine operation in aeroelastic wind turbine models, e.g. for control system design or structural design of the wind turbine. The main disturbances in this case are typically wind variations and gravity, including the periodic components due to the rotation of the blades.

The second order model, shown in Figure 13, includes the dynamics of the active power controller, but assumes that the rotor current responds instantaneously, i.e. $\vec{i}_r=\vec{i}_r^{\,ref}$. The output of the active power controller is the q-component i_{rq} of the rotor current. Since the rotor speed is an input to the generator model, coming from HAWC2, the implemented reduced order DFIG model is presented in Figure 14.

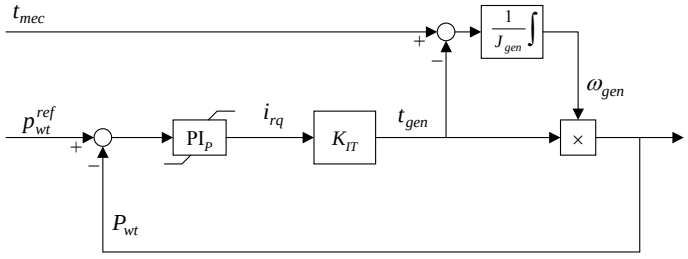

Figure 13 Block diagram of 2nd order DFIG model [17]

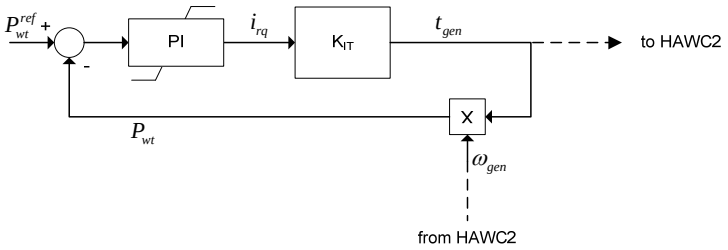

Figure 14 Block diagram of the implemented DFIG model

In Figure 13 it is illustrated that the generator torque t_{gen} is a constant K_{IT} multiplied by i_{rq}. This can be seen using the following according to [17]:

$$t_{gen}=3N_{pp}L_m\,\mathrm{Im}\left(\vec{i}_s\cdot\vec{i}_r^{\,*}\right) \quad (25)$$

where $\vec{i}_r^{\,*}$ in (25) is the complex conjugated of $\vec{i}_r$. In [15], (25) is used with motor sign of i_s, whereas we use generator sign. Thus, in [15], the calculated torque is the motor

torque, while in our case t_{gen} is the torque with generator sign. In [15], (25) was used to derive K_{IT} assuming motor sign and that the number of pole pairs N_{pp}=1. Applying the similar approach with generator sign and N_{pp} pole pairs, K_{IT} is obtained according to

$$K_{IT} = \frac{t_{gen}}{i_{rq}} \cong \sqrt{3} N_{pp} \frac{U_{sn}}{\omega_{en}} \frac{X_m}{X_s + X_m} \tag{26}$$

In (26), the generator stator resistance R_s is neglected, and the grid is assumed to be ideal with rated stator voltage U_{sn} and rated grid pulsation ω_{en}. In that case, K_{IT} is constant. X_m is the main reactance and X_s is the stator leakage reactance in the standard steady state T-equivalent diagram, presented in Figure 15. These data are usually available from the standard data sheets.

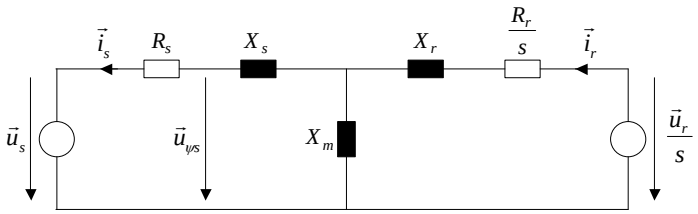

Figure 15 Standard T steady state equivalent diagram of the doubly-fed induction generator

This model considers only the active power control, which interacts strongly with the mechanical system. The reactive power is omitted, because the reactive power only has a marginal influence on the mechanical system.

5 Simulations results

5.1 Fixed speed wind turbine

5.1.1 Steady-state generator model

The block diagram of the implemented fixed speed wind turbine with a squirrel-cage induction generator is presented in Figure 16. The input to the *Slip Generator* DLL is the rotor speed and the output is the mechanical torque.

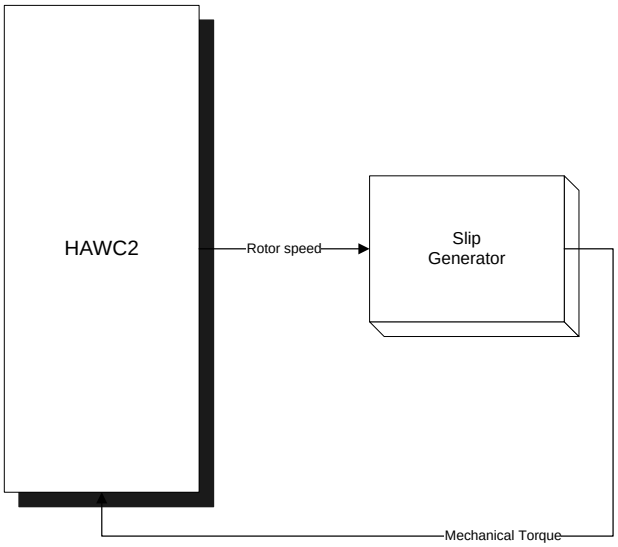

Figure 16 Block diagram of the fixed speed wind turbine with slip generator

The simulations conducted aimed at assessing the operation of the fixed speed wind turbine with the slip generator. The wind turbine is a fixed speed with passive aerodynamic stall. A set of step response simulations with deterministic wind speed (no turbulence, no tower shadow) is performed. The wind speed varies from 5 to 13 m/s with 1 m/s step every 20 sec. In Figure 17 the typical quantities versus time are shown: wind speed in [m/s], generator torque in [p.u.], generator speed in [p.u.] and generator power in [p.u.].

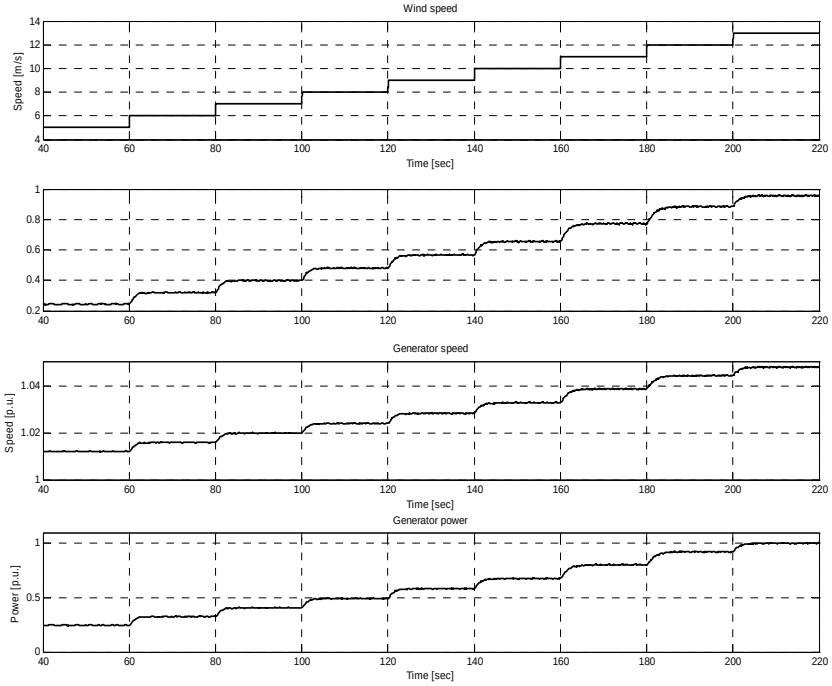

Figure 17 Simulation results for wind steps

5.1.2 Dynamic generator model

The block diagram of the fixed speed wind turbine with dynamic model of the squirrel cage induction generator simulation model is illustrated in Figure 18.

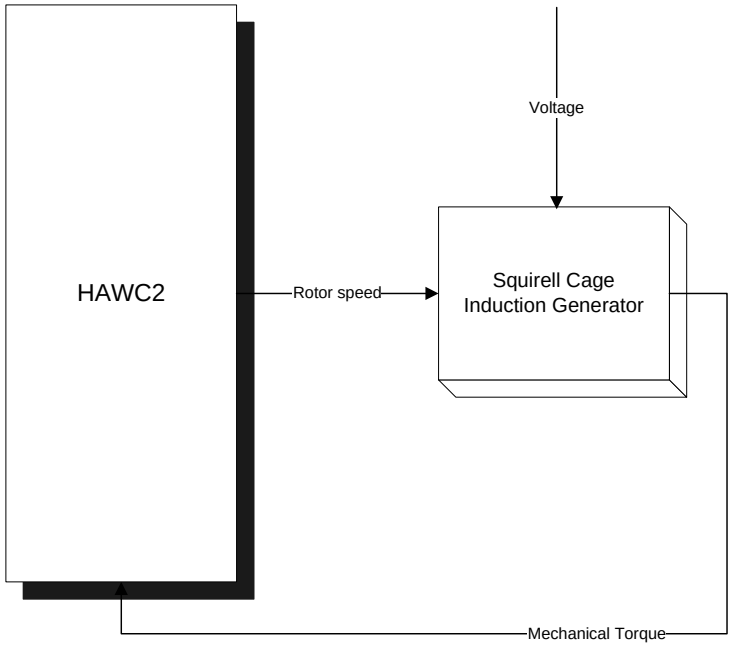

Figure 18 Fixed speed wind turbine with squirell cage induction generator

In this case, the inputs to the *Squirrel Cage Induction Generator* DLL are the rotor speed (coming from HAWC2) and the stator voltages, in *dq*, defined in the configuration file. The rotor voltages are also inputs in the model. They are kept to zero in this simulation. By adding the rotor side control, the model is extended to DFIG.

Since the model includes two differential equations (rotor fluxes) and since the numerical solver integrated in HAWC2 can not, so far, be accessed by the external DLLs, the fourth order Runge-Kutta ODE solver was implemented.

The simulations conducted aimed at assessing the operation of the fixed speed wind turbine with the dynamic squirrel cage induction generator model. The wind turbine is a fixed speed with passive aerodynamic stall. A set of step response simulations with deterministic wind speed (no turbulence, no tower shadow) is performed. The wind speed varies from 5 to 13 m/s with 1 m/s step every 20 sec. In Figure 19 the typical quantities versus time are shown: wind speed in [m/s], generator torque in [p.u.], generator speed in [p.u.] and generator power in [p.u.].

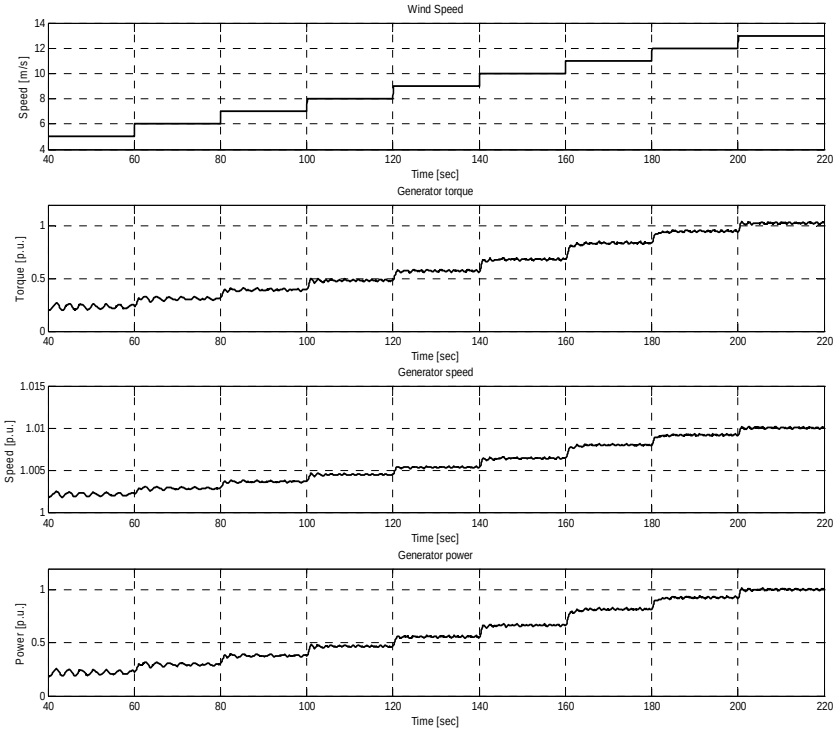

Figure 19 Simulation results for wind steps

The active and reactive power is shown in Figure 20. As expected, the generator is drawing reactive power from the grid.
The rotor fluxes and currents are shown in Figure 21 and in Figure 22, respectively.

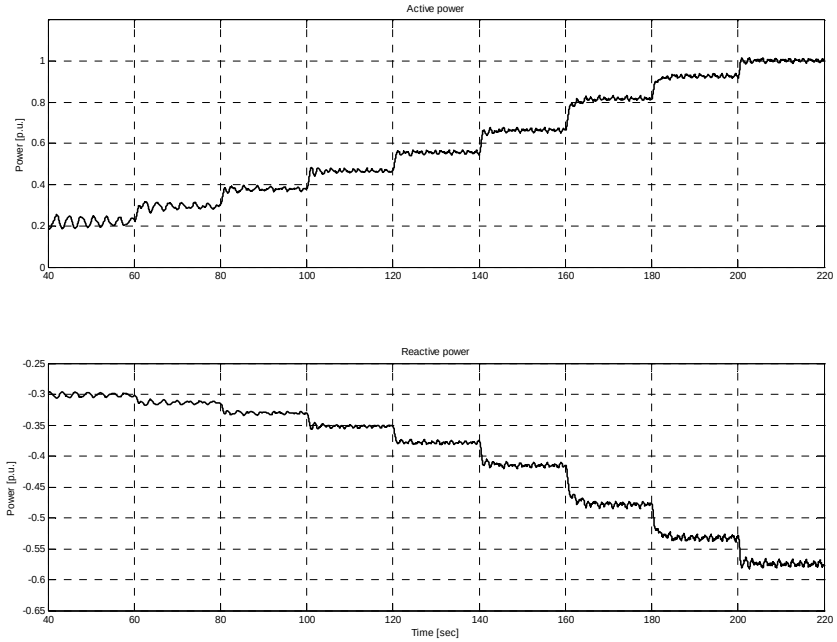

Figure 20 Active and reactive power

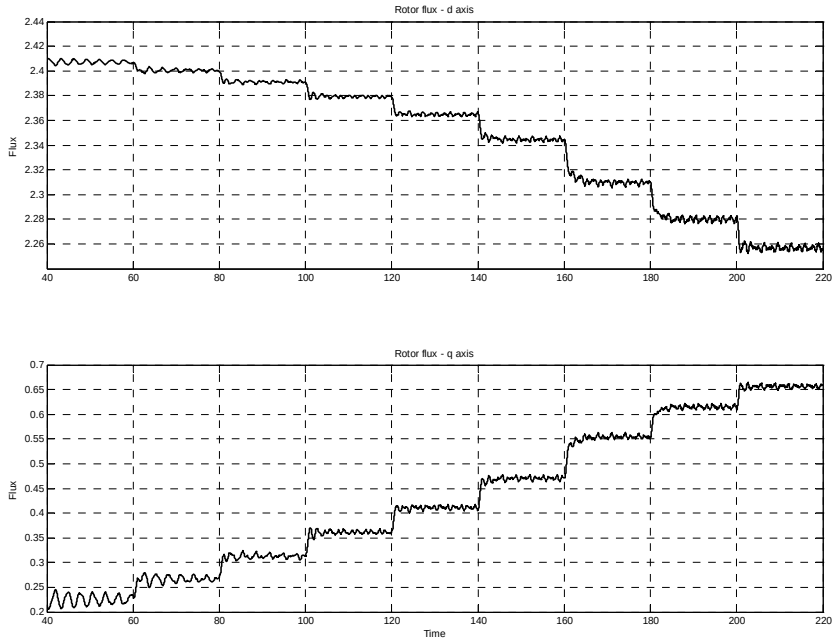

Figure 21 Rotor fluxes

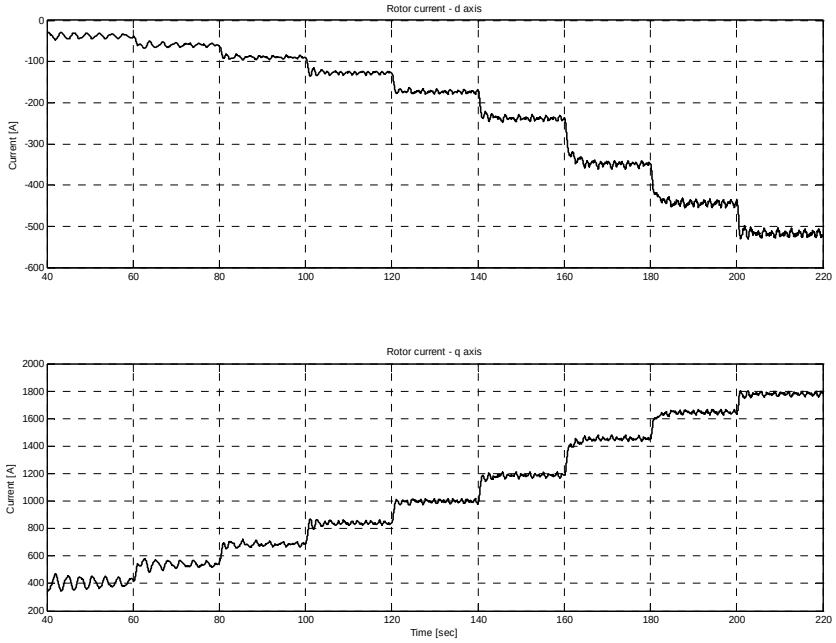

Figure 22 Rotor currents

Finally, the stator currents are shown in Figure 23.

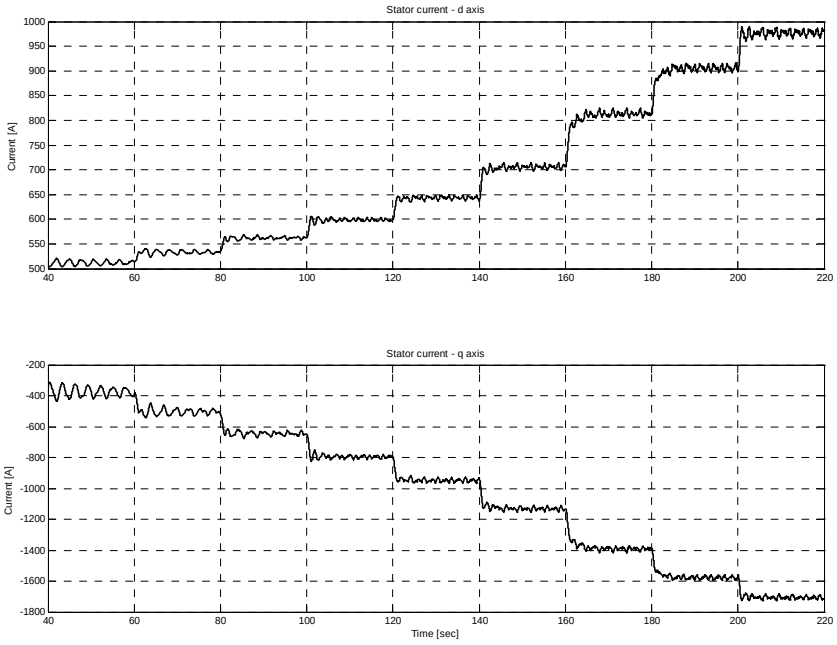

Figure 23 Stator currents

5.2 Variable speed wind turbine

5.2.1 Pitch controller

In variable pitch wind turbines, the aerodynamic power is limited using a PI-regulator that adjusts the reference pitch angle based on the error between rotational speed and rated speed. The PI-regulator has a minimum setting of zero deg, which makes the turbine operate with zero pitch angles at low wind speeds.

A special gain scheduling to adjust for increased effect of pitch variations at high wind speed compared to lower speeds is applied. This gain scheduling handles the linear increasing effect of $dP/d\theta$ with increasing wind speed and pitch angle. This gain function is implemented following the expression:

$$gain(\theta) = 1/1 + \theta/KK \tag{27}$$

where the value *KK* is the pitch angle where $dP/d\theta$ has increased by a factor of 2 [2].

To increase the gain when large rotor speed error occurs another gain function is applied to the PI-regulator. This gain function is simply 1.0 when the rotor speed is within 10 % of rated speed and 2.0 when the error exceeds 10 %. This very simple gain function seems to limit large variations of the rotational speed at high wind speed.

The pitch servo is modelled as a 1st order system with a time constant of 0.2 s. The maximum speed of the pitch movement is set to 10 deg/s [2].

The control diagram is presented in Figure 24. The input is the measured rotor speed ω_{rot} and outputs are the reference power $P_{e,ref}$ and the collective pitch angle $\theta_{col,ref}$.

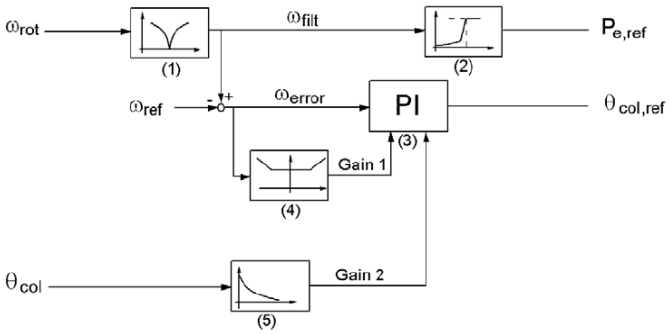

Figure 24 Control diagram of pitch control and power reference [2]

5.2.2 Steady – state generator model

The block diagram of the variable speed wind turbine with simple generator simulation model is illustrated in Figure 25. The generator model used is the one presented in §4.1.2.

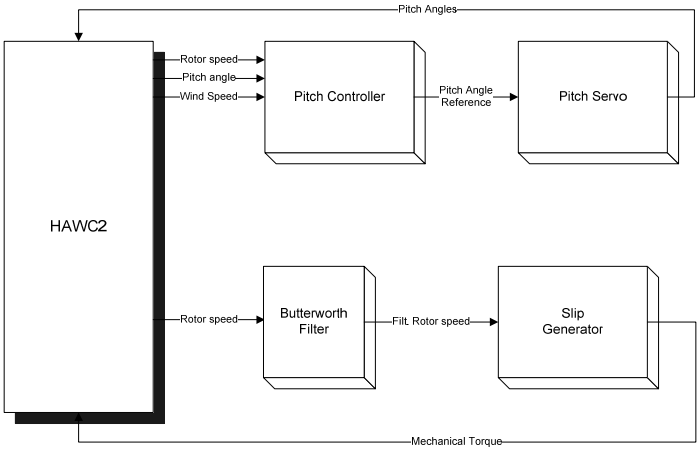

Figure 25 Variable speed wind turbine with slip generator simulation scheme

The pitch servo is modelled as a 1st order system with a time constant of 0.2 sec. The maximum speed of the pitch movement is set to 20 deg/s.

In order to asses the developed model, a set of step response simulations with deterministic wind speed (no turbulence, no tower shadow) is performed. The wind speed is increased with 1 m/s every 40 sec, from 5 to 20 m/s. In Figure 26 and Figure 27 the results of the step simulation are shown, with the typical quantities versus time: wind speed in [m/s], generator torque in [p.u.], generator speed in [p.u.], generator power in [p.u.] and pitch angle in [deg].

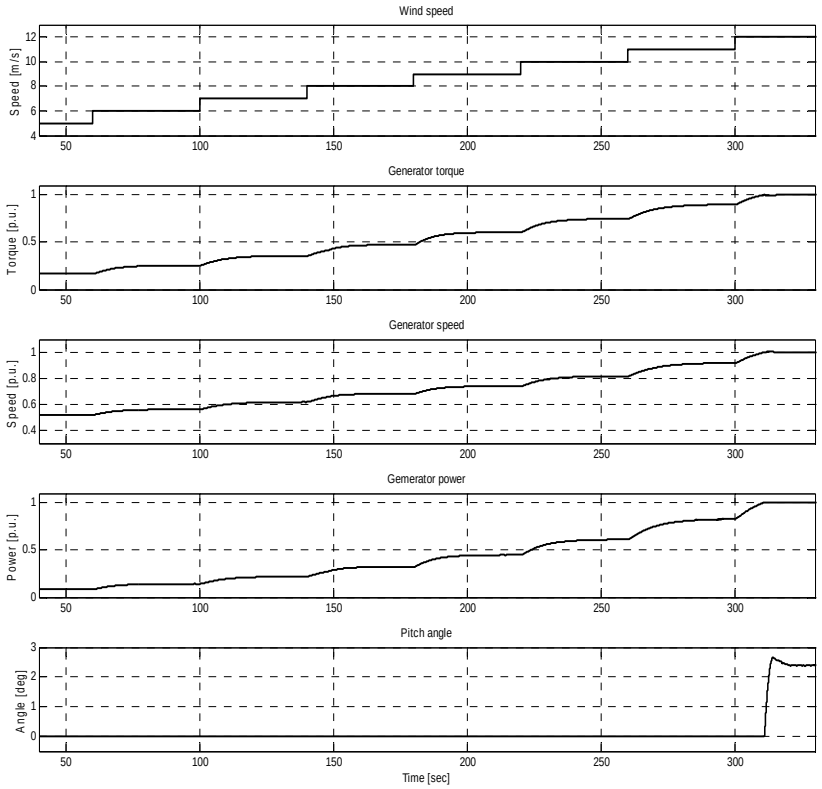

Figure 26 Step in wind speed from 5 to 12 m/s

Figure 27 Step in wind speed from 12 to 20 m/s

At low wind speeds, the pitch controller keeps the pitch angle constant at zero degrees and the speed varies. It should be noted that it takes quite some time (> 30 sec) for the rotational speed to reach the new level. This could lead to a suboptimal value of the rotational speed in turbulent wind.

At high wind speeds, the pitch controller modifies the pitch angle in such way that the rotational speed varies around the rated value. The dynamic evolution of the rotational speed is almost identical over the whole wind speeds range (12 to 20 m/s). This shows that the gain scheduling is working properly.

5.2.3 Dynamic generator model

The block diagram of the variable speed wind turbine with DFIG is presented in Figure 28.

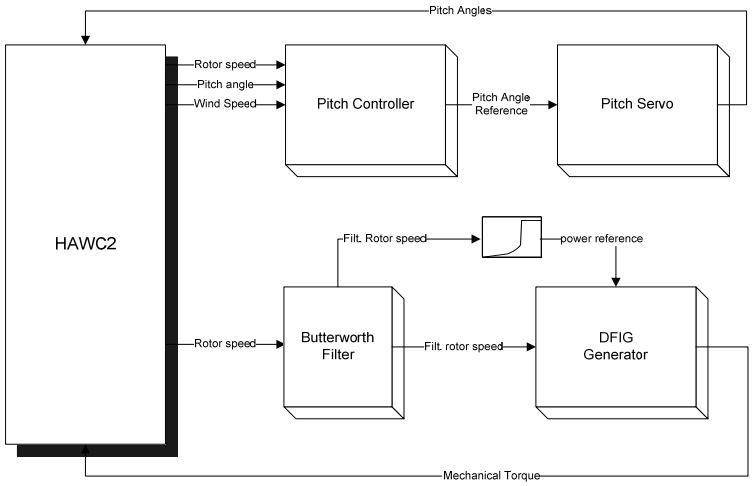

Figure 28 Variable speed wind turbine with DFIG simulation scheme

The power reference is calculated using a predefined power – speed characteristic, presented §4.2.2. The input is the filtered rotor speed.

In order to asses the developed model, a set of step response simulations with deterministic wind speed (no turbulence, no tower shadow) is performed. The wind speed is increased with 1 m/s every 40 sec, from 5 to 20 m/s. In Figure 29 and Figure 31 the results of the step simulation are shown, with the typical quantities versus time: wind speed in [m/s], generator torque in [p.u.], generator speed in [p.u.], generator power in [p.u.] and pitch angle in [deg]. In Figure 30 and in Figure 32, the rotor current on the q – axis is presented.

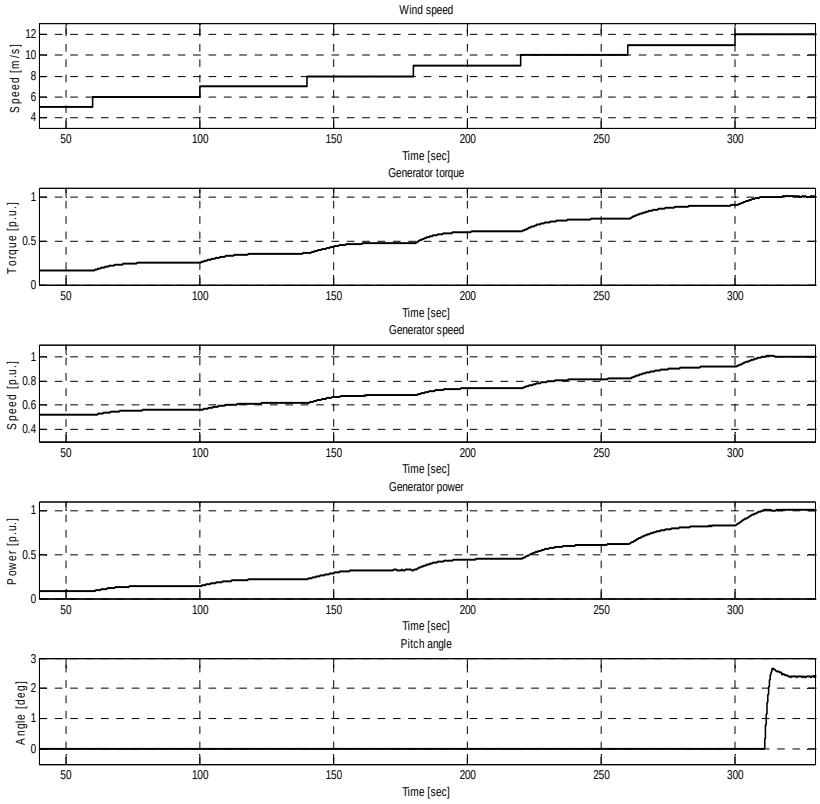

Figure 29 Step in wind speed from 5 to 12 m/s

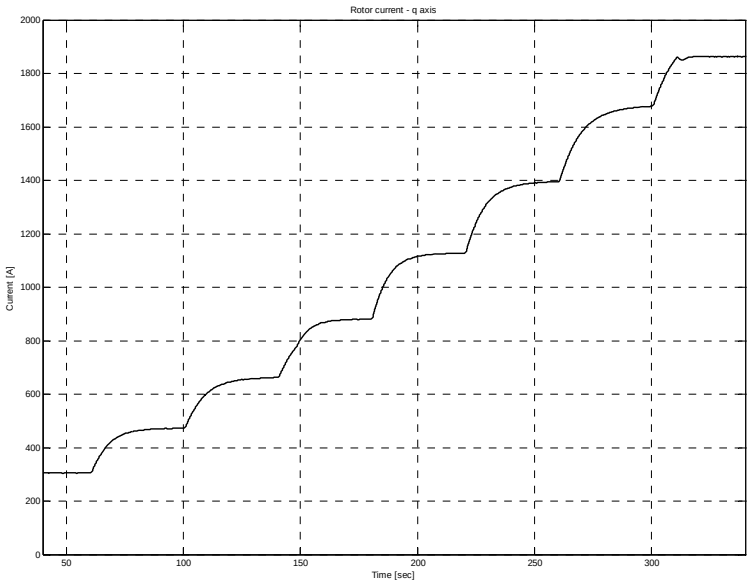

Figure 30 Step in wind speed from 5 to 12 m/s, rotor current on the q-axis

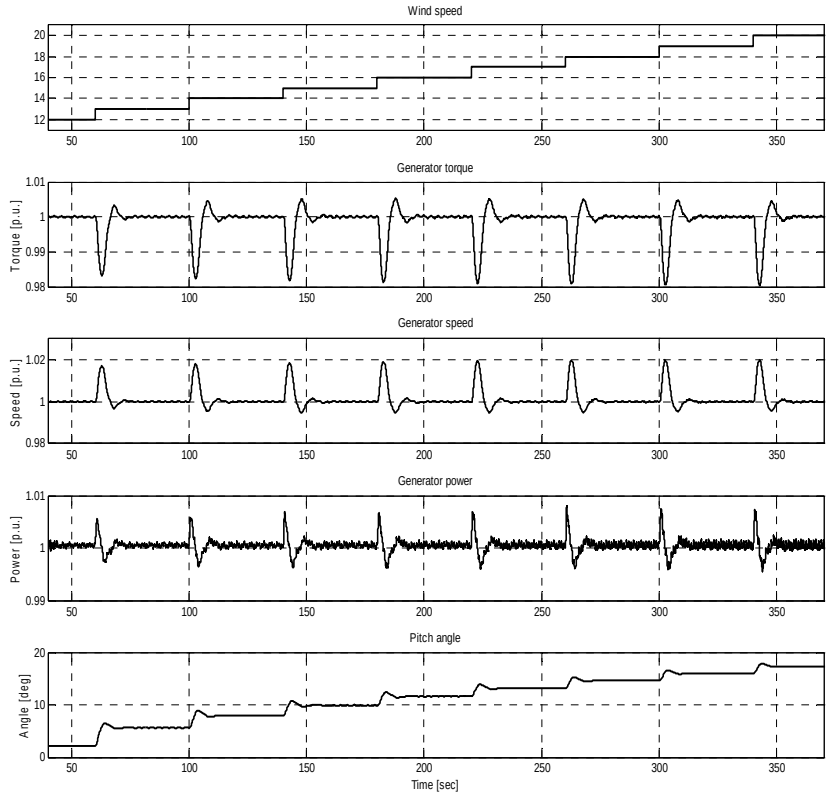

Figure 31 Step in wind speed from 12 to 20 m/s

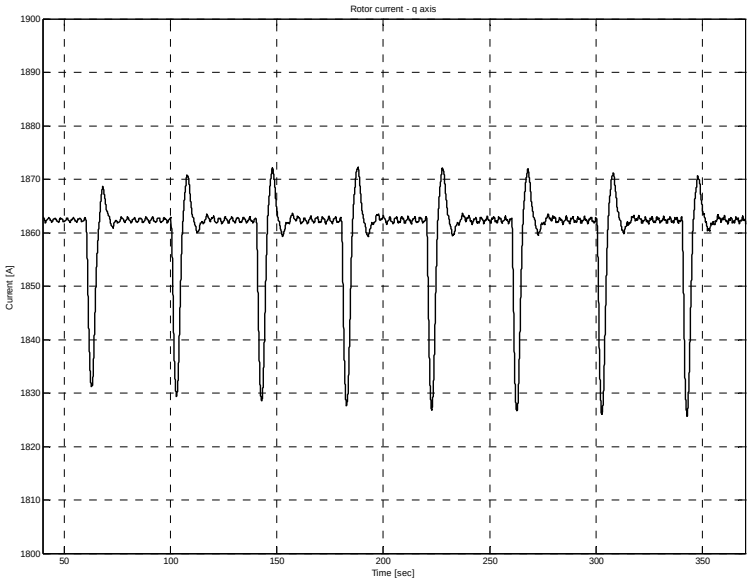

Figure 32 Step in wind speed from 12 to 20 m/s, rotor current on the q-axis

At low wind speeds, the pitch controller keeps the pitch angle constant at zero degrees and the speed varies. It should be noted that it takes quite some time (> 30 sec) for the

rotational speed to reach the new level. This could lead to a suboptimal value of the rotational speed in turbulent wind.

At high wind speeds, the pitch controller modifies the pitch angle in such way that the rotational speed varies around the rated value. The dynamic evolution of the rotational speed is almost identical over the whole wind speeds range (12 to 20 m/s). This shows that the gain scheduling is working properly.

6 Conclusions

The work presented is this report is a first step towards developing an electric components library to be used with Risø's aerolaestic code HAWC2. The code has been constantly developed and improved - currently being at version 3.45, thus a significant effort has been put into keeping the library up to date.

The possibility to investigate the interaction and the influence between the mechanical and the electrical parts of a wind turbine is becoming more and more important. The requirements for wind turbines to stay connected to the grid during and after voltage sag imply potential challenges in the design of wind turbines, both for mechanical structure and electrical system. Thus, it is very important to develop models of the electrical components that can be used in aero elastic codes and allow to quantify the loads' impact on the wind turbines' lifetime, during and after grid faults.

The electrical components library for use with HAWC2 includes both steady state and dynamical models for fixed and variable speed wind turbines.

A simple steady-state slip model was developed for the fixed speed wind turbine. This model is suitable for aeroelastic design of wind turbines under normal operation.

A dynamic model of an induction generator for the fixed speed wind turbine was developed. The model includes the dynamics of the rotor fluxes and can be easily extended to the DFIG model, by including the control of the rotor voltages (inputs to the model). The model is suitable for a more detailed investigation of the mechanical – electrical interaction, both under normal and fault operation.

For the variable speed wind turbine, a steady-state model, typically used in aeroelastic design, was implemented. The model can be used for normal and, to some extent, for fault operation. The reduced order dynamic model of a DFIG was implemented. The model includes only the active power controller and can be used for normal operation conditions.

Some of the models presented in this report will be used in other research projects. In the European project UPWIND, Work Package 1.2, HAWC2 simulations of a fixed speed wind turbine with both steady-state and dynamic model will be conducted. Similar, in the PSO project entitled "Grid fault and design-basis for wind turbines" HAWC2 simulations will be conducted.

7 References

[1]. Petersen JT. *Kinematically nonlinear finite element model of a horizontal axis wind turbine*. Risø National Laboratory, Roskilde, Denmark, Risø, Jul. 1990

[2]. Larsen TJ, Hansen MH, Iov F. *Generator dynamics in aeroelastic analysis and simulations*. Risø-R-1395(EN), Risø National Laboratory, July 2003.

[3]. S. Oeye, *Dynamic stall simulated as a time lag of separation*, Proc. 4th IEA Symp. on Aerodynamics of Wind Turbines, Rome, 1991.

[4]. Leishmann, J.G., Beddoes, T.S, *A Semi-Empirical Model for Dy-namic Stall, Journal of the American Helicopter Society. 1986.*

[5]. Larsen TJ. *Description of the DLL regulation interface in HAWC*. Risø-R-1290(EN), Risø National Laboratory, 2001.

[6]. Mann J. *Wind field simulation*. Prob. Eng. Mech. 13 (4) (1998) 269-282.

[7]. http://www.waspengineering.dk/

[8]. Veers PS. *Three-dimensional wind simulation*. SAND88-0152. Sandia National Laboratories. Albuquerque 1988

[9]. http://www.ieawind.org/Annex_XXIII.html

[10]. http://www.upwind.eu

[11]. Hansen AD, Jauch C, Sørensen P, Iov F, Blaabjerg F. *Dynamic wind turbine models in power system simulation tool DIgSILENT*. Risø-R-1400(EN), Risø National Laboratory, December 2003.

[12]. Hansen A.D. *Generators and Power Electronics for wind turbines*. Chapter in "Wind Power in Power systems", John Wiley&Sons, Ltd, 24 p., 2004.

[13]. Burton T, Sharpe D, Jenkins N. and Bossanyi E. *Wind Energy Handbook*. John Wiley & Sons, New-York 2001.

[14]. Hansen AD, Iov F, Blaabjerg F, Hansen LH. *Review of contemporary wind turbine concepts and their market penetration*. Wind Eng. (2004) **28**, 247-263.

[15]. Leonhard, W. *Control of electrical drives*, Springer Verlag, 2001. ISBN 3540418202.

[16]. Iov F., Hansen AD, Sørensen P, Blaabjerg F. *Wind Turbine Blockset in Matlab/SIMULINK*. Technical Report, Aalborg University, March 2004.

[17]. Sørensen P, Hansen AD, Lund T, Bindner H. *Reduced models of doubly fed induction generator system for wind turbine simulations*. Wind Energy (2006) **9**, 299-311

Risø's research is aimed at solving concrete problems in the society.

Research targets are set through continuous dialogue with business, the political system and researchers.

The effects of our research are sustainable energy supply and new technology for the health sector.